Capacitance hysteresis in GaN/AlGaN heterostructures

L. E. Byrum,[1] G. Ariyawansa,[1] R. C. Jayasinghe,[1] N. Dietz,[1] A. G. U. Perera,[1,a)] S. G. Matsik,[2] I. T. Ferguson,[3] A. Bezinger,[4] and H. C. Liu[4]
[1]Department of Physics and Astronomy, Georgia State University, Atlanta, Georgia 30303, USA
[2]NDP Optronics LLC, Mableton, Georgia 30126, USA
[3]School of Electrical and Computer Engineering, Georgia Institute of Technology, Atlanta, Georgia 30032, USA
[4]Institute for Microstructural Sciences, National Research Council, Ottawa K1A 0R6, Canada

(Received 9 September 2008; accepted 3 December 2008; published online 26 January 2009)

Capacitance characteristics with voltage and frequency of n^+-GaN/$Al_xGa_{1-x}N$ heterojunction ultraviolet (UV)-infrared (IR) photodetectors are reported. A distinct capacitance step and capacitance hysteresis have been attributed to trap energy states located just above the Fermi level at the GaN/AlGaN interface, most likely due to N-vacancy and/or C-donor impurities. The presence of the hysteresis is due to the accumulation of charge at the heterointerface, which is dependent on the location of the continuum of interface trap states relative to the Fermi level. The Al fraction in the barrier layer has been found to significantly change the positions of the interface trap states relative to the Fermi level. © *2009 American Institute of Physics*. [DOI: 10.1063/1.3068179]

I. INTRODUCTION

The wide band gap of GaN (3.4 eV) makes GaN-based devices relatively resistant to thermal carrier emission and interband tunneling.[1] Although the GaN/AlGaN material system is structurally stable and relatively resistant to cracking, the lattice mismatch at interface junctions hinders the growth of high quality devices. Trap states have been found to form at GaN/AlGaN heterointerfaces due to disturbances in crystal periodicity, dangling bonds, interface roughness, and lattice dislocations.[2] The presence of these interface trap states introduces auxiliary capacitance and conductance components in parallel with the detector's intrinsic capacitance, thus altering photogenerated responsivity.

The detector operates by the excitation of carriers when UV and/or IR radiation are incident on a sample. The IR detection is based on the intraband transitions from the n^+-GaN emitter,[1] while UV detection is based on interband transitions in the AlGaN barrier.[3] A thorough discussion of the detection mechanisms can be found elsewhere.[3] Variations in barrier layer Al content and contact layer doping concentration will change the UV and IR threshold. However, increased Al content has been found[2] to contribute to the number of interface trap states due to increased lattice strain at the heterojunction.

II. EXPERIMENT

The detectors were grown by low pressure metal-organic chemical vapor deposition on a *c*-plane sapphire substrate. As shown in Fig. 1, the structures consist of a 0.2 μm n^+-doped GaN top contact (emitter) layer, a 0.6 μm $Al_xGa_{1-x}N$ barrier layer, and a 0.7 μm n^+-doped GaN bottom contact layer. The $Al_xGa_{1-x}N$ barrier layers in the 1547 and 1158 series had Al fractions of 0.1 and 0.026, respectively. The top and bottom contact layers in both sample series were n^+-doped with silicon to a doping concentration of 5×10^{18} cm^{-3}.

Capacitance-voltage (*C-V*) and capacitance-frequency (*C-f*) measurements were carried out using a computer controlled Hewlett-Packard 4284A *LCR* meter. Capacitance scans were run between −2 and +2 V with the top contact biased and the bottom contact grounded at frequencies ranging from 100 Hz to 1 MHz.

III. RESULTS AND DISCUSSION

Capacitance steps in the *C-V* curves of the 1547 series, shown in Fig. 2, are believed to result from the abrupt change in carrier trap occupation due to N-vacancy and C-donor defect energy states located slightly above the Fermi level at the n^+-GaN/AlGaN interface. These carrier trap states most likely have an energy band associated with them, as opposed to a discrete energy state. As shown in the band

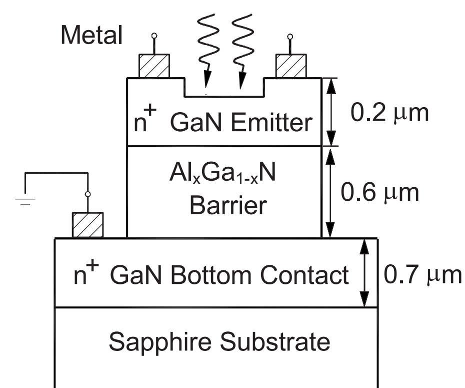

FIG. 1. The structure of the detector consists of an undoped $Al_xGa_{1-x}N$ barrier layer located between n^+-GaN top and bottom contact layers. The 1547 and 1158 samples had Al fractions of 0.1 and 0.026, respectively. When the sample is negatively biased, the top contact layer will act as an emitter. Both n^+-GaN layers were doped with Si to a concentration of 5×10^{18} cm^{-3}.

a)Electronic mail: uperera@gsu.edu.

 © 2009 American Institute of Physics

Downloaded 27 Jan 2009 to 131.96.4.51. Redistribution subject to AIP license or copyright; see http://jap.aip.org/jap/copyright.jsp

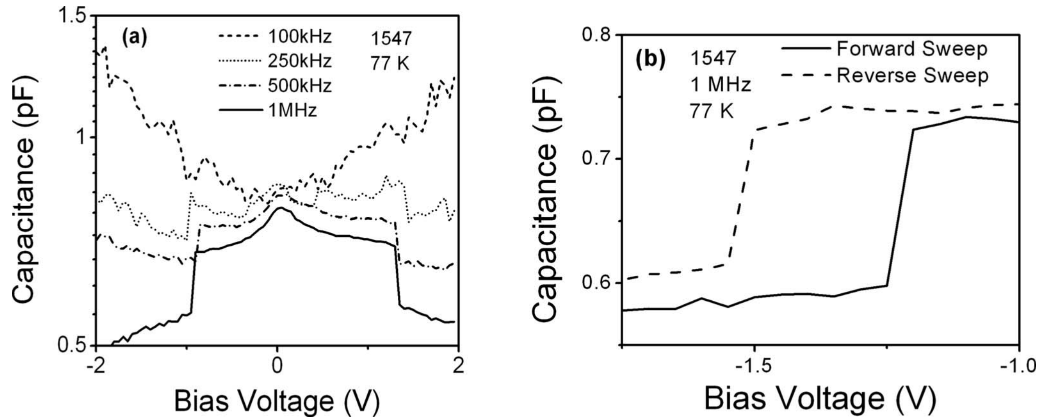

FIG. 2. Capacitance-voltage scans of the 1547 series showing (a) frequency-dependent capacitance dispersion and a capacitance step. The capacitance step became more pronounced as frequency increased. (b) The capacitance hysteresis between forward and reverse sweeps. The vertical offset between forward and reverse sweeps is within the noise range.

diagrams of the 1547 sample at zero bias, Fig. 3(a), trap states above the Fermi level are empty; but when the bias reaches a critical value, shown in Fig. 3(b), the Fermi level enters the previously unoccupied trap state bands. Thus, carriers can readily move in and out of the trap states, leading to an increase in capacitance. Conversely, when the Fermi level sweeps out of the occupied trap state bands, the capacitance suddenly decreases, as the trap states can no longer contribute to capacitance.

Simulated results[4] indicate that trap state relaxation time constants for generation and recombination processes are dependent on carrier concentration. The electron recombination (capture) relaxation time τ_r and the electron generation (emission) relaxation time τ_g are

$$\tau_r = (\sigma_n v_{\mathrm{th}} n)^{-1} \tag{1}$$

and

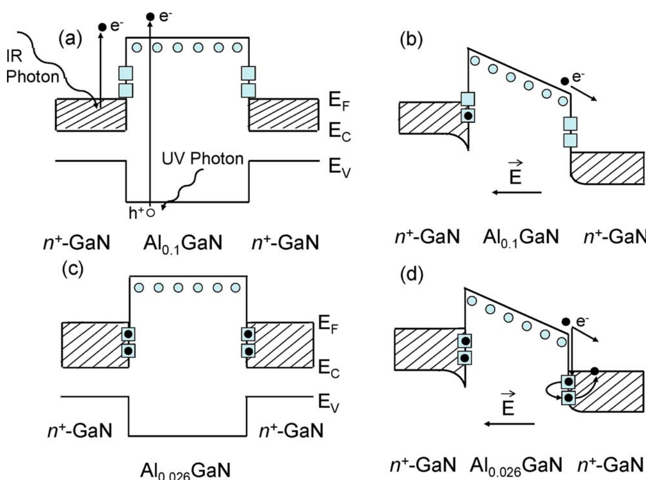

FIG. 3. (Color online) Band diagram for the 1547 series at (a) zero bias showing the detection mechanism of the dual-band detectors and (b) negative bias. At zero bias the C-donor and N-vacancy trap states were located above the Fermi level. As the bias became more negative, the Fermi level swept through the interface trap states, causing the abrupt increase/decrease in capacitance. Band diagram for the 1158 series with (c) zero bias and (d) negative bias. When the 1158 sample was negatively biased the C-donor and N-vacancy trap states were located below the Fermi level. The work function Δ was 88 meV for the 1158 series and 200 meV for the 1547 series.

$$\tau_g = (\sigma_n v_{\mathrm{th}} n_1)^{-1}, \tag{2}$$

where σ_n is the capture cross section for electrons, v_{th} is the thermal velocity, and n is the nonequilibrium concentration of mobile electrons,

$$n = n_i \exp\left(\frac{e[\phi_{F_n} - \phi]}{k_B T}\right), \tag{3}$$

and n_i is the intrinsic density

$$n_1 = N_C \exp\left(\frac{[E_C - E_t]}{k_B T}\right), \tag{4}$$

where e and k_BT denote the electron charge and thermal energy at a specific temperature, respectively. Both expressions are of similar form; however, the nonequilibrium concentration n depends on the intrinsic density and the quasi-Fermi potential of the electrons ϕ_{F_n} and the electrical potential of the work function ϕ, whereas n_1 depends on the effective electron density of states N_C and the position of the trap state energy E_t relative to the conduction band edge E_C. Thus, n_1 and τ_g are not susceptible to bias induced band bending.[4]

The hysteresis in the C-V curves for the 1547 series, shown in Fig. 2(b), can be explained as follows. With a forward sweep, the N-vacancy and C-donor impurity states are initially empty. These energy states act as acceptor-like electron trap states. As the bias increases the Fermi level will sweep through the trap states, thus filling the trap states and causing an abrupt change in carrier concentration. As these trap states become occupied, negative charges will build up at the interface, resulting in an accumulation region. When the sweep direction is reversed, the C-donor and N-vacancy trap states are initially filled. The charge in the accumulation region leads to lower effective fields at the interface and, hence, a higher required voltage for the capacitance step, which occurs as the Fermi level sweeps out of the energy continuum and the trap states are abruptly emptied. The difference in initial carrier occupation of the C-donor and N-vacancy trap states between a forward and reverse sweep results in the observed hysteresis.

At low carrier concentrations the trap state relaxation times are still fast enough to respond, so although an abrupt

Downloaded 27 Jan 2009 to 131.96.4.51. Redistribution subject to AIP license or copyright; see http://jap.aip.org/jap/copyright.jsp

capacitance step will occur, the trap states can emit carriers fast enough to prevent a significant buildup of charges at the interface. At sufficiently high carrier concentrations, the relaxation times of the energy states decreases to a point where the charging process can no longer follow the voltage modulation. Since carriers captured in the trap states cannot be emitted fast enough, a residual charge will remain at the interface when the sweep direction is reversed, resulting in the capacitance hysteresis.

The presence of interface frequency-dependent trap states was responsible for the observed capacitance dispersion in the *C-V* profiles. Frequency-dependent capacitance dispersion has been observed[2,5] in other GaN/AlGaN heterojunction structures in the 10 kHz–1 MHz regions with corresponding relaxation time constants of 1 and 63 μs, respectively. Trap state relaxation times in the 1547 series could be calculated from the *C-f* profile, and ranged from 68 to 107 μs at 77 K. A single relaxation time cannot be identified[4] because relaxation times are dependent on carrier concentration [see Eq. (1)], rather a broad range of relaxation times is observed. Relaxation times measured between 50 and 166 K were used to construct an Arrhenius plot. A single energy state was identified with a thermal activation energy of 14.7 ± 1.2 meV. Similar thermal activation energies of 12–17 meV for shallow Si-donor impurities in GaN have been reported.[6]

In the *C-f* scans of the 1547 series, the measured capacitance for all bias values approached the geometrical capacitance of the structure as the frequency was increased. This is a result of the carrier transport process reaching a maximum value due to finite inertia when the frequency exceeds the inverse relaxation time.[7] Additionally, at high frequencies and low bias, the voltage changes too rapidly for impurities to react. As the frequency decreases, impurity trap states have time to become charged and the capacitance begins to increase.

IR spectroscopy of the 1547 series, see Fig. 4, showed impurity related absorption centers with activation energies of 30.9 ± 0.1, 149 ± 1, and ~ 189 meV. A summary of the trap states, Al fraction, and corresponding work functions in the 1547 and 1158 series are shown in Table I. The defect energy state with an activation energy of 30.9 ± 0.1 meV was attributed to shallow Si-donor impurities in the AlGaN barrier layer. C-donor and/or N-vacancy impurities at the heterojunction accounted for the trap states with activation energies of 149 ± 1 and ~ 189 meV. The activation energies of these trap states indicate that they are located at the heterointerface, just above the Fermi level (200 meV).

Based on previous reports,[8–10] the three impurity related absorption centers at 30.8 ± 0.2, 125 ± 1, and 140 ± 2 meV in the IR spectra of the 1158 series, shown in Fig. 4, were determined to be Si-donor and N-vacancy/C-donor impurities. The activation energies of the C-donor and N-vacancy impurities indicate that the defect energy states are located at the heterointerface, just below the Fermi level (88 meV).

The peak corresponding to shallow Si-donor impurities in the AlGaN barrier was present in both the 1547 and 1158 series with the same activation energy, indicating that while

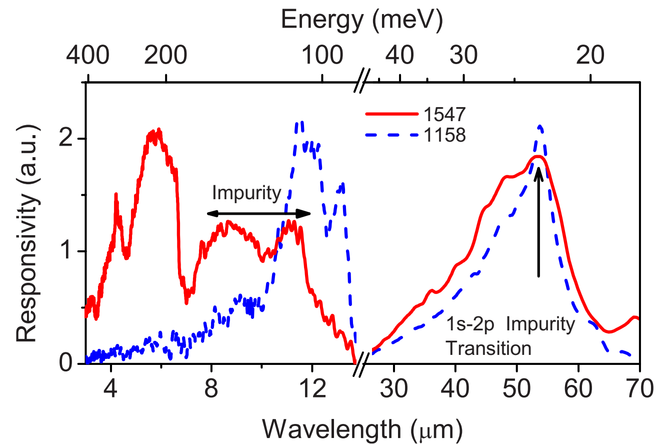

FIG. 4. (Color online) IR spectra showing impurity related absorption centers in the 1547 and 1158 series. In the 1547 series N-vacancy and/or C-donor centers with transitional energies of 112 ± 0.5 and ~ 142 meV corresponding to activation energies of 149 ± 1 and ~ 189 meV, respectively; and Si-donor impurities had $1s$-$2p$ transitional energy of 23.2 ± 0.1 meV. In the 1154 series N-vacancy and/or C-donor transitional energies of 93.4 ± 0.5 and 105 ± 1.5 meV, corresponding to activation energies of 125 ± 1 and 140 ± 2 meV, respectively; and Si-donor impurities $1s$-$2p$ transitional energy of 23.1 ± 0.1 meV.

the barrier Al fraction does change the barrier height and location of interface trap states, it does not affect the location of shallow Si-donor impurities.

Based on *C-V* and *C-f* measurements from samples with different Al concentrations in the barrier layer, the same trap states appear to be present. However, the mechanism in which these trap states respond to an applied bias was distinctly different, as the Al fraction alters the conduction band offset[11] and the position of the Fermi level changes with respect to the trap state energy levels. The most likely cause for this discrepancy is the difference in Al concentration in the barrier; 1547 samples have an Al fraction of 0.1, while the 1158 samples have an Al fraction of 0.026. Barrier layer Al concentration contributes to the conduction band offset at the n^+-GaN/$Al_xGa_{1-x}N$ heterojunction. Band diagrams of the 1547 and 1158 series under zero and negative applied bias, including potential trap states, are shown in Fig. 3. The work function Δ in the 1547 series (at 200 meV) resulted in the Fermi level lying just below the C-donor and N-vacancy energy bands. Thus, an applied bias allowed the Fermi level to sweep through the trap states, producing the capacitance step and capacitance hysteresis. However, the decreased Al

TABLE I. Summary of sample parameters and impurity activation energies. In the 1547 series, all impurity trap states were located above the Fermi level, whereas in the 1158 series, all impurity trap states were located below the Fermi level.

	Sample No.	
	1547	1158
Al fraction	0.10 ± 0.001	0.026 ± 0.001
Work function (meV)	200 ± 2	88 ± 2
Si-donor (meV)	30.9 ± 0.1	30.8 ± 0.2
N-vacancy (meV)	149 ± 1	125 ± 1
C-donor (meV)	~ 189	140 ± 2

Downloaded 27 Jan 2009 to 131.96.4.51. Redistribution subject to AIP license or copyright; see http://jap.aip.org/jap/copyright.jsp

fraction in the 1158 samples positioned the C-donor and N-vacancy trap states below the Fermi level (88 meV). Because the trap states in the 1158 series were consistently below the Fermi level, the trap states did not go through the process of the Fermi level sweeping through either the initially filled or initially empty (depending on scan direction) trap states; thus, there was no observed capacitance step or capacitance hysteresis in the *C*-*V* scans of the 1158 series. Rather, the presence of trap states below the Fermi level in the 1158 series resulted in negative capacitance due to an impact ionization-like process at the heterointerfaces. A more detailed discussion of the mechanisms responsible for negative capacitance in the n^+-GaN/$Al_{0.026}$GaN heterostructure can be found elsewhere.[12]

IV. CONCLUSION

In summary, multiple carrier trap states in n^+-GaN/$Al_xGa_{1-x}N$ heterojunction photodetectors were characterized based on capacitance data. The capacitance hysteresis was attributed to the accumulation of charge at the heterointerface, when C-donor and/or N-vacancy defect energy states were present at the interface just above the Fermi level. The conditions required for the capacitance step are similar to that of a capacitance hysteresis. These impurities can be integrated into the heterostructure during the growth process, such as the use of organic precursors.[3] The Al fraction in the barrier layer was found to strongly influence the capacitance characteristics of the samples, as the Al fraction in the barrier layer not only changed the work function at the interface but, more importantly, changed the position of the interface trap states relative to the Fermi level.

ACKNOWLEDGMENTS

This research was supported in part by the U.S. Air Force under Small Business Innovation Research Program (SBIR) (Contract No. FA9453-06-C-005) and the Georgia Research Alliance. The authors would like to acknowledge Dr. Dave Cardimona and Dr. Bill Glass for fruitful discussions.

[1] G. Ariyawansa, M. B. M. Rinzan, M. Strassburg, N. Dietz, A. G. U. Perera, S. G. Matsik, A. Asghar, I. T. Ferguson, H. Luo, and H. C. Liu, Appl. Phys. Lett. **89**, 141122 (2006).
[2] R. M. Chu, Y. G. Zhou, K. J. Chen, and K. M. Lau, Phys. Status Solidi C **0**, 2400 (2003).
[3] G. Ariyawansa, M. B. M. Rinzan, M. Alevli, M. Strassburg, N. Dietz, A. G. U. Perera, S. G. Matsik, A. Asghar, I. T. Ferguson, H. Luo, A. Bezinger, and H. C. Liu, Appl. Phys. Lett. **89**, 091113 (2006).
[4] T. Lindner, G. Paasch, and S. Scheinert, J. Appl. Phys. **98**, 114505 (2005).
[5] W. L. Liu, Y. L. Chen, A. A. Balandin, and K. L. Wang, J. Nanoelectron. Optoelectron. **1**, 258 (2006).
[6] W. Gotz, N. M. Johnson, C. Chen, H. Liu, C. Kuo, and W. Imler, Appl. Phys. Lett. **68**, 3144 (1996).
[7] A. G. U. Perera, W. Z. Shen, M. Ershov, H. C. Liu, M. Buchanan, and W. J. Schaff, Appl. Phys. Lett. **74**, 3167 (1999).
[8] W. J. Moore, J. A. Freitas, and R. J. Molnar, Phys. Rev. B **56**, 12073 (1997).
[9] M. Sumiya, K. Yoshimura, K. Ohtsuka, and S. Fuke, Appl. Phys. Lett. **76**, 2098 (2000).
[10] V. Bougrov, M. Levinshtein, S. Rumyantsev, and A. Zubrilov, *Properties of Advanced Semiconductor Materials* (Wiley, New York, 2001).
[11] A. Salvador, G. Liu, W. Kim, O. Aktas, A. Botchkarev, and H. Morkoc, Appl. Phys. Lett. **67**, 3322 (1995).
[12] L. E. Byrum, G. Ariyawansa, R. C. Jayasinghe, N. Dietz, A. G. U. Perera, S. G. Matsik, I. T. Ferguson, A. Bezinger, and H. C. Liu, IEEE Trans. Electron Devices (submitted).

Downloaded 27 Jan 2009 to 131.96.4.51. Redistribution subject to AIP license or copyright; see http://jap.aip.org/jap/copyright.jsp